Spectral analysis of the gravity and elevation along the western Africa–Eurasia plate tectonic limit: Continental versus oceanic lithospheric folding signals

A. Muñoz-Martín [a,*], G. De Vicente [a], J. Fernández-Lozano [a], S. Cloetingh [b], E. Willingshofer [b], D. Sokoutis [b], F. Beekman [b]

[a] Grupo de Tectonofísica Aplicada. Universidad Complutense de Madrid, Spain
[b] Faculty of Earth and Life Sciences, Vrije Universiteit Amsterdam, The Netherlands

Keywords:
Lithospheric folding
Spectral analysis
Eurasia-Africa plate tectonic boundary
Elevation
Gravity

A B S T R A C T

Large-scale folding is a key mechanism of lithospheric deformation and has been described in many parts of the Earth, both for the continental and oceanic lithospheres. Some aspects of this process such as the presence of coupling/decoupling between the crustal deformation and the mantle lithosphere, or between different lithospheres, make it necessary to accurately control the periodic characteristics of the elevation and of the gravity signal. 1D spectral analysis of gravity and topography profiles is sensitive to a series of factors: the location, length and orientation of the profiles, as well as the number of samples taken. We carry out a systematic analysis of the periodicities in the topography and gravity, both 1D and 2D, along the western border of the Africa–Eurasia plate tectonic boundary. We analyze the sensitivity of the 1D and 2D spectral analysis in order to compare the results along a plate boundary where oceanic and continental lithospheres are in contact with different tectonic, kinematic and rheological aspects.

Our 1D spectral results indicate that the greater the profile length, the longer the wavelength peaks that are found. Nevertheless there are some periodic signals that appear in almost all the analyzed profiles: 100–250 km for the N–S profiles across oceanic plate boundary and 150–250 km where the plate boundary is developed over continental lithospheres. The 2D spectral analysis avoids the problems found in relation to the particular location of the profile but the resulting wavelengths are slightly higher than those obtained from the 1D spectral analysis. The wavelengths estimated for both oceanic and continental lithospheres at the Africa–Eurasia boundary (>250 km) show low values of mean mantle strength ($<10^{13}$ Pa m).

The presence of lithospheric folds means that the continental and oceanic lithospheres are mechanically coupled. This had previously been suggested for Iberia but not for the limit between S Iberia and the Terceira Triple Junction.

The orientation of the lithospheric folds is NW–SE at the contact between continental lithospheres and NNE–SSW at the contact between oceanic lithospheres. This difference is also reflected in the signal anisotropy and must be related to the rotation of the tectonic stresses in the same direction. A large periodic signal (wavelength >600 km) was also detected both in 1D and 2D spectral results. After drawing the filtered values, the resulting maps indicate that this signal is related to the transition between continental and oceanic lithospheres and to the significant changes in crustal and/or lithospheric thickness from the Mid-Atlantic Ridge to the continental margins of western Eurasia.

1. Introduction

The observation of regular patterns of large-scale deformation belts, together with similar signals in the gravity anomaly and elevation, related to the kinematics and dynamics of the main tectonic plates,has led different authors (e.g. Cloetingh et al., 1999, 2002; Stephenson and Cloetingh, 1991; Lambeck, 1983; McAdoo and Sandwell, 1985; Ziegler et al., 1995; Nikishin et al., 1993; Bonnet et al., 2000; Gerbault, 2000; Krishna et al., 2001) to put forward a process of deformation through buckling of the entire lithosphere (known as lithospheric folding). These have been found within intraplate settings, both in continental lithosphere (Brittany, Iberia, Artic Canada, Central Asia, Alps, and Pannonian Basin) and in oceanic lithosphere (Indian Ocean).

The Iberian Peninsula and the NW corner of Africa (Fig. 1) is characterized by a series of topographic highs and associated depressions. Despite a clear periodicity between mountain ranges from N to S, little is known about the mechanism or mechanisms involved in intraplate mountain building. Recently, Verges and Fernandez (2006), argued that the observed topography was the

Please cite this article as: Muñoz-Martín, A., et al., Spectral analysis of the gravity and elevation along the western Africa–Eurasia plate tectonic limi..., Tectonophysics (2010), doi:10.1016/j.tecto.2010.09.036

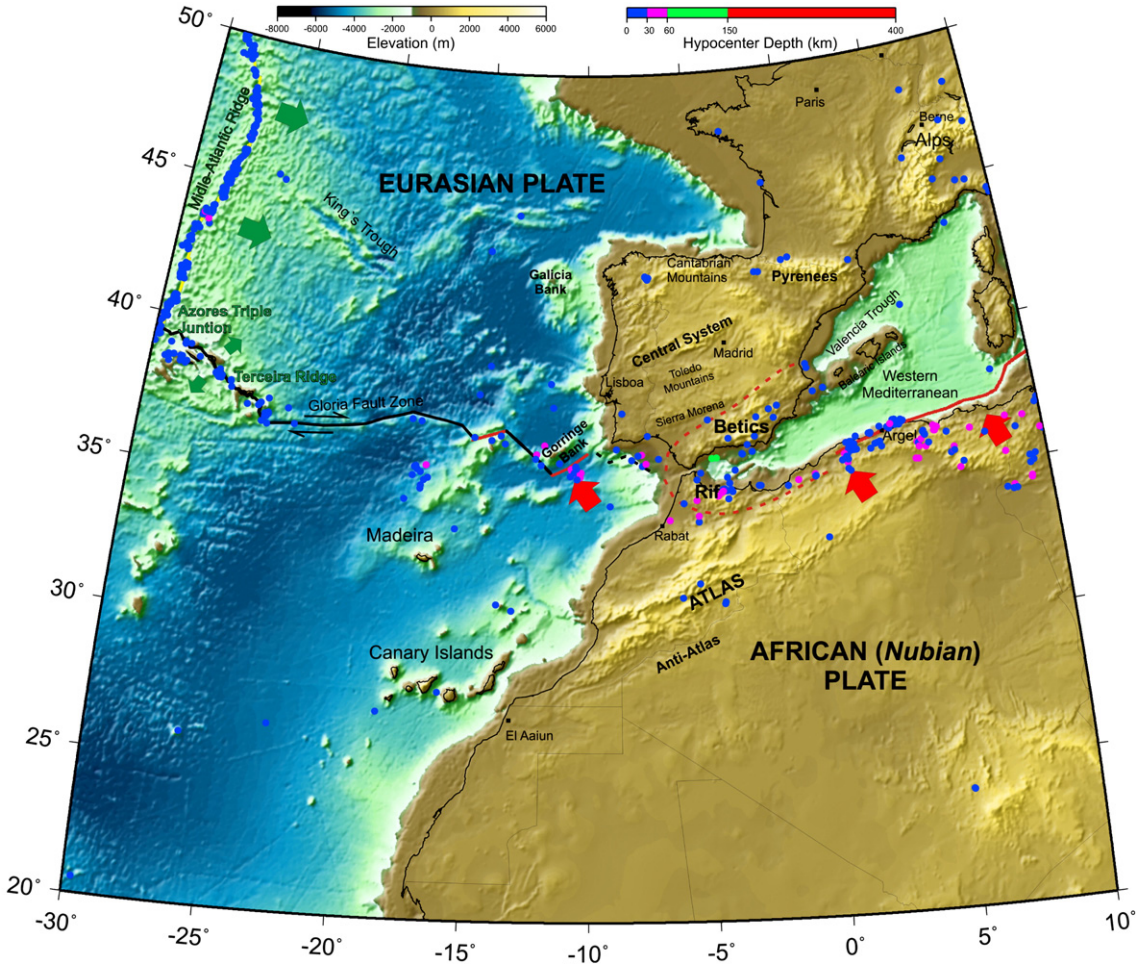

Fig. 1. Simplified tectonic map of the western Africa–Eurasia plate boundary superimposed on the topography extracted from GTOPO30 and GEBCO, 2003 databases. Broken lines indicate, approximately, tectonic boundaries, microplates and block limits (modified from De Vicente and Vegas, 2009). Red arrows indicate the Present-Day collisional push between Africa and Eurasia, and green arrows the Mid-Atlantic Ridge push. Colour dots show epicenters and focal depths from the EHB Bulletin (International Seismological Centre, 2009). (For interpretation of the references to color in this figure legend, the reader is referred to the web version of this article.)

result of several episodes of compression (during the Alpine Orogeny) and extension (back-arc extension in the western Mediterranean domain through most of the Miocene times). Unlike the above mentioned authors, Cloetingh et al. (2002) have proposed a mechanism of lithosphere folding, that is based on the observation of regular patterns at deformation belts, along with the correlation between gravity anomalies and elevation, related to the plate kinematics and dynamics within intraplate settings.

The mechanism of lithospheric folding invokes particular thermo-mechanical conditions in order to allow large-scale deformation. The rheological stratification of the continental lithosphere is strongly dependent on rheology, distribution of heat in depth and crustal thickness (Ranalli, 1995; Schmalholz et al., 2009; Sonder and England, 1986). With these assumptions, the strength of the continental lithosphere would be influenced by both, the lithosphere mantle and the crust. Whereas in the oceanic lithosphere, the tectono-thermal age of the lithosphere would control the mechanism of deformation (McAdoo and Sandwell, 1985; Cloetingh et al., 1999). Furthermore, the total strength of the oceanic lithosphere would be mostly influenced by the strength in the mantle (Fig. 2). Although little is known about the steady-state of the continental lithosphere in Iberia, Tejero and Ruiz (2002) have shown the strength profiles from the main plate interior. Their results predict a brittle mantle below the Duero and Tagus Basins and a relatively weak mantle under the Spanish Central System. Similar results were obtained in central and southwest Iberia by Stapel (1999). Moreover, recent data compiled by Fullea et al. (in press), reveal large variations in the depth of the Moho and the lithosphere–asthenosphere boundary without any correlation between their thicknesses in southern Spain and the Moroccoan Atlas.

Under these conditions, several numerical modelling and analogue experiments (Cloetingh et al., 2002; Schmalholz et al., 2002, 2009; Martinod and Davy, 1994; Sokoutis et al., 2005; Luth et al., 2010; Fernández-Lozano et al., in press), have shown that the mechanism of folding in active regions would be enabled by a low strain rate (dependent on the strength of the mantle) and the effective transmission of stress across the plate interior (Andeweg et al., 1999; de Vicente and Vegas, 2009). Moreover, widespread deformation would facilitate the transmission of the fold trend along the northern part of the African Atlas which in turn may explain the high altitude reached by the Atlas Mountains (de Lamotte et al., 2009; de Vicente and Vegas, 2009; Ghorbal et al., 2008; Teixell et al., 2003).

Such lithospheric folds show different wavelengths depending on the rheological properties of the deformed lithosphere and its tectono-thermal age (Fig. 2) (McAdoo and Sandwell, 1985; Cloetingh et al., 1999, 2002). The presence of previous faults and/or thermal anomalies originating in the mantle also in many cases localize the deformation. The main feature of the lithospheric folds is that they strike perpendicular to the maximum compression direction of the active tectonic stresses during the Plio-Quaternary in Iberia (Cloetingh et al., 2002).

Please cite this article as: Muñoz-Martín, A., et al., Spectral analysis of the gravity and elevation along the western Africa–Eurasia plate tectonic limi..., Tectonophysics (2010), doi:10.1016/j.tecto.2010.09.036

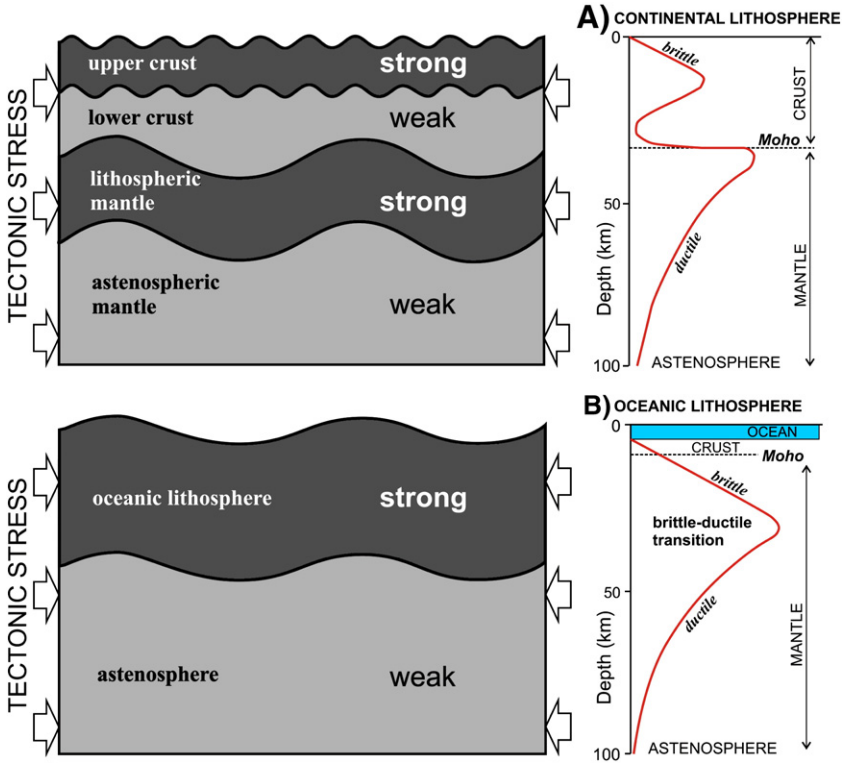

Fig. 2. Conceptual model for lithospheric folding development for continental (upper) and oceanic (lower) lithospheres under horizontal tectonic stress. Typical strength profiles are shown for: a) two layers continental crust and b) normal oceanic crust.

Generally speaking, these types of large-scale structures can be analyzed by examining the contrast between the natural prototype (a sufficiently large area of deformed lithosphere) and a series of suitably-scaled numerical and analogue models. The prototype is mainly characterized by means of 1D spectral analysis of topographic and gravity profiles transversal to the major tectonic structures observable in the upper crust. An alternative approach is to analyze the geological surfaces that can be deduced from seismic profiles.

Numerical modelling of lithospheric folding is generally undertaken using thermo-mechanical models along 2D vertical cross sections (McAdoo and Sandwell, 1985; Beekman et al., 1996; Burov and Cloetingh, 1997; Burov and Poliakov, 2001; Cloetingh et al., 2002; Schmalholz et al., 2009), as well as with plain strain models that incorporate the elastic deformation of the lithosphere and processes of erosion and sedimentation with the development of drainage systems (García-Castellanos, 2002). More recent experiments on these types of structures are using lithospheric-scale analogue models (Martinod and Davy, 1994; Sokoutis et al., 2005; Luth et al., 2010; Fernández-Lozano et al., in press). These incorporate vertical and horizontal variations in the rheological properties of the lithosphere and in the sub-lithospheric mantle. The discussion of the origin of the lithospheric folding and the processes that control its development is then based on a comparison of the prototype and the models.

The results of these papers confirm the widespread presence of whole-lithosphere folds and constrain the factors that control their development. However, some of the results, such as the presence of coupling/decoupling between the crustal deformation and the mantle lithosphere, or between different lithospheres, make it necessary to accurately control the periodic characteristics of the elevation and of the gravity signal. 1D spectral analysis of gravity and elevation profiles is an approach that is sensitive to a series of factors: the location, length and orientation of the profiles, as well as the number of samples taken (measuring pixel).

We have carried out systematic analysis of the periodicities in elevation and gravity along the western border between the African and Eurasian plates (both 1D and 2D) as outlined in the previous work (Cloetingh et al., 2002). Our study zone was chosen on the grounds that it represents a very well known plate limit from a kinematic and dynamic point of view (Serpelloni et al., 2007; De Vicente and Vegas, 2009), making it possible to compare the prototype and the numerical and analogue model results (Cloetingh et al., 2002; Fernández-Lozano et al., in press).

Our main objective is therefore to analyze the sensitivity of the 1D and 2D spectral analyses in order to determine the periodicities of elevation and gravity signals and to compare the results along a plate boundary where oceanic and continental lithospheres are in contact. Finally, the results obtained from the spectral analysis are compared with the spatial distribution of the lithospheric folds, the anisotropy of the lithosphere and tectonic, kinematic and rheological aspects.

2. Tectonic setting and Present-Day stress field

The paleo-reconstructions of the movement of Africa with respect to Iberia during the Tertiary (Rosenbaum et al., 2002) have shown that between the anomalies of An 13 and An 6 (Early Oligocene–Lower Miocene), Africa and Iberia came 115 km closer, which implies an N–S approximate shortening of 3–4% with a rate lower than 1 cm per year (Fig. 3A). Paleomagnetic studies (Palencia, 2004) indicate that no important relative motion, in a paleomagnetic sense, has occurred at the boundary between Africa and the Iberian Peninsula since the Eocene. During this time, most of the convergence between both plates was resolved through deformations which affected the upper crust and the lithosphere, giving rise to higher order folds and the basic topographical pattern, both on and off shore (Figs. 1, 3). Thereafter, boundary stresses responsible for the Cenozoic deformation of Iberia and northwestern Africa from Eocene up to Middle–Upper Miocene, must be referred to the Iberia–Europe interface, the Cantabrian–Pyrenean border with a main N–S orientation.

This structural pattern is lost between the C6 and C5 anomalies (Lower Miocene–Upper Miocene), where the paleomagnetism indicates

Please cite this article as: Muñoz-Martín, A., et al., Spectral analysis of the gravity and elevation along the western Africa–Eurasia plate tectonic limi..., Tectonophysics (2010), doi:10.1016/j.tecto.2010.09.036

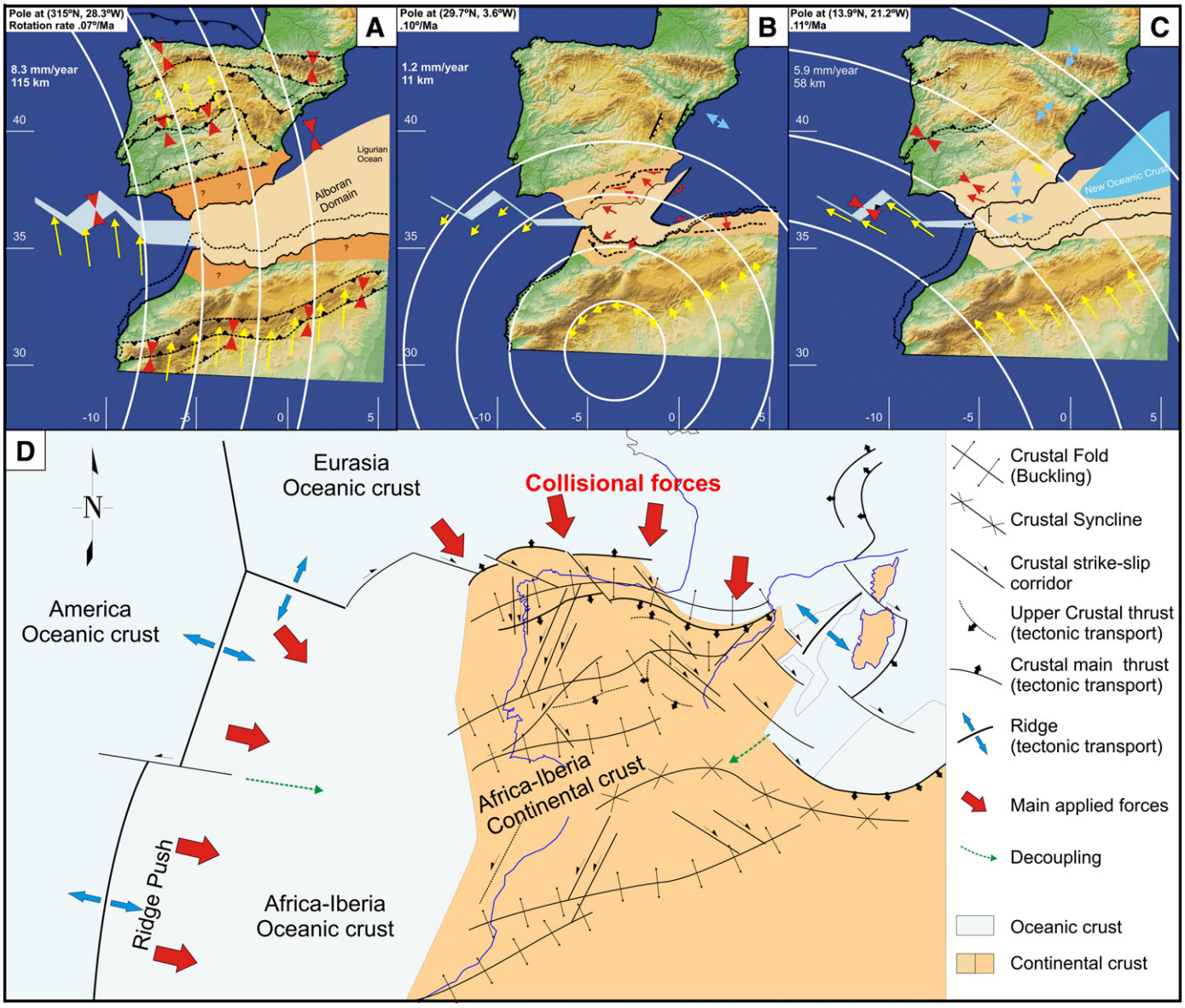

Fig. 3. A–C: Paleopoles of Iberia–Africa movement during the Cenozoic (modified from Rosenbaum et al., 2002). A) Relative Africa–Iberia movement between An 13–An 6: Iberia moored to Africa. B) Relative movement between Africa–Iberia An 6–An 5: Iberia–Africa decoupling. C) Relative movement between Africa–Iberia An 5–Present day: Iberia is a part of Eurasia. Red arrows: shortening. Blue arrows: extension. Yellow arrows: mean displacements. D) Paleo-plates sketch for lithospheric folding development (modified from De Vicente and Vegas, 2009). (For interpretation of the references to color in this figure legend, the reader is referred to the web version of this article.)

that the movement between Africa and Iberia was right lateral and parallel to the plate boundary, although at a very low velocity (1.2 mm per year) (Rosenbaum et al., 2002) (Fig. 3B). From a tectonic point of view, this sharp change in plate kinematics can be interpreted as the ceasing of the constrictive conditions of the deformation and the end of the active lithosphere folding on a board scale. The coincidence in time with the displacement of the Alboran Block towards the West implies that this emplacement mechanically decoupled Iberia from Africa (De Vicente and Vegas, 2009).

The current kinematics between Iberia and Africa involves a convergence in the NW–SE direction, which is shown in the state and the orientation of the active stresses (De Vicente et al., 2008) (Fig. 3C). This new stress field is superimposed on the structures generated up to the Lower Miocene and does not have its origin in the northern Edge (Pyrenees), where mainly normal type focal mechanisms are registered (Olaiz et al., 2009). A new Africa–Europe plate boundary was created to the south of the Iberian Peninsula and its formation is still ongoing (De Vicente and Vegas, 2009).

2.1. Present-Day stress field

To characterize the actual stress field in the study area we have applied the methodology published by Olaiz et al. (2009) to the area investigated, including focal mechanism data up to December, 2009. The used data sources are earthquake focal mechanisms calculated from the centroid moment tensor inversion (Dziewonski et al., 1982) from different catalogues: CMT catalogue (Dziewonski and Woodhouse, 1983), the Italian INGV (Pondrelli et al., 2002, 2004), the ETH-Zürich (Braunmiller et al., 2002), the Ibero–Maghrebian moment tensor project at IAG-Granada (Stich et al., 2003), and finally the IGN-Madrid catalogue (Rueda and Mezcua, 2005).

For the calculation of the orientation and the shape factor of the strain–stress ellipsoid we have applied the methodology proposed by De Vicente (1988), based on the "slip model of tri-axial deformation" (Reches, 1983). The method provides a value of the shape factor of the strain ellipsoid ($k' = ey/ez$, ey maximum horizontal shortening, ez vertical axis) and the maximum horizontal shortening trend (Dey) for

Please cite this article as: Muñoz-Martín, A., et al., Spectral analysis of the gravity and elevation along the western Africa–Eurasia plate tectonic limi..., Tectonophysics (2010), doi:10.1016/j.tecto.2010.09.036

every individual focal mechanism. To map the direction of maximum horizontal shortening (Dey) we use the values obtained from the "Slip Model", except in the case of the extensional focal mechanisms on the oceanic ridges, where we have plotted Dex (maximum horizontal extension), because of the "ridge push" effect. The value of the k′ ratio varies between +∞ (radial constriction) and −∞ (radial stretching). We have re-sized these values to a scale between 0 and 300. To map the strain–stress regime, the individual k′ values heterogeneously distributed, were first filtered calculating a mean value in 1515-minute-size blocks. This was made to avoid aliasing short wavelengths. Then we interpolated the mean k′ value to a 15-minute regular mesh by using kriging and a linear variogram (Fig. 5) and, finally, this grid was resampled to a final 1-degree regular grid.

The obtained final map (Fig. 5) shows that from the Azores Triple Junction towards the west, Dey shows a progressive rotation from E–W to WNW. Between the Azores Triple Junction and the area North of Algeria the map shows a smooth rotation in the Dey orientation: from WNW to N–S, with some local variations in the S of the Iberian microplate, probably associated with the emplacement towards the W of the Alboran–Betics–Rif system (Vázquez and Vegas, 2000; De Vicente et al., 2008).

Results for the Dey distribution orientations in the Eurasian Plate interior show that E–W trends predominate in the Atlantic Ocean near the MAR. This notion confirms the key role of the oceanic lithosphere in the transmission of stresses, as suggested by its high integrated strength (Tesauro et al., 2007; Stuwe, 2007). In general, the horizontal stresses rotate inside Europe from an E–W trend near the Mid-Atlantic Ridge, towards an NW orientation to the east. This general pattern has also been recognized by previous authors (Müller et al., 1992). The major variations in this general trend are located in the Pyrenees (Dey's rotation towards E–W, related to the presence of the ancient plate limit between Iberia and Eurasia).

The strain–stress regime distribution in Europe displays a good correlation with the main tectonic features and with the topography (Fig. 5). The extensional zones are clearly dominant along the Mid-Atlantic Ridge. To the east of the Azores triple junction the strain regime continues to be extensional along the Gloria Fault, up to the area of the Gorringe Bank characterized by the thrusting of oceanic crust (Vázquez and Vegas, 2000), where it changes to compression. This important oceanic crustal-scale thrusting marks the beginning of the convergent limit along the contact between Eurasia and Africa in the S of Europe. This convergent limit is defined by a broad band with complex geometry that goes from the SW of Iberia up to the N of Tunis. This band shows reverse and strike–slip earthquakes, though there are also zones with extensional stresses that disconnect the continuity of the shortening zone.

Inside the European plate, an extensional close to strike–slip strain regime is dominant, with well delimited areas with extensional or compressive regime. In this way, an intraplate extensional zone appears in the Pyrenees, that shows an extension perpendicular to the mean topographic trend of the chain. This fact has been interpreted as an isostatic compensation of the topography (De Vicente et al., 2008).

The fact that NW Africa appears in compresión must be related with the compressional focal mechanisms along the Atlas, and with the lack towards the south. In this sense the compressional regime south of the Atlas can be considered as an artificial effect of the interpolation.

3. Elevation and gravity data

The selected study zone is located at the western edge of the African–Eurasian plate boundary, between latitude 20° to 50°N and longitudes from the mid-Atlantic Ridge (30°W), at the triple junction of the Azores–Terceira Ridge, to Corsica, Sardinia and western Algeria (10°E) (Figs. 1, 4). Both the types of lithosphere and the deformation regime and style vary along the boundary from East to West. In the most westerly part the plate boundary is located between oceanic lithospheres, first with an extensional regime (Azores), then a strike–slip regime (Azores–Gibraltar fault zone) and finally with a compressive regime at the Gorringe Bank and SW Iberia (Fig. 5).

This change is associated with increasing magnitudes of the displacement vector of the African plate with respect to Eurasia, as well as the S_{HMAX} rotations resulting from the location of the Eurasia–Africa rotation pole shown in Fig. 3 (Rosenbaum et al., 2002; Serpelloni et al., 2007; De Vicente et al., 2008; De Vicente and Vegas, 2009). Further east the contact between European and African lithospheres is diffuse due to the effect of the Alborán Domain (microplate), which brings about a more widely distributed deformation along a series of intraplate basement uplifts (De Vicente and Vegas, 2009). Towards the east the boundary again becomes better defined and is located along the northern coast of Morocco and the Tell Mountains in Algeria, with an active compressive tectonic stress regime (Fig. 5). This variation along the plate boundary is reflected in

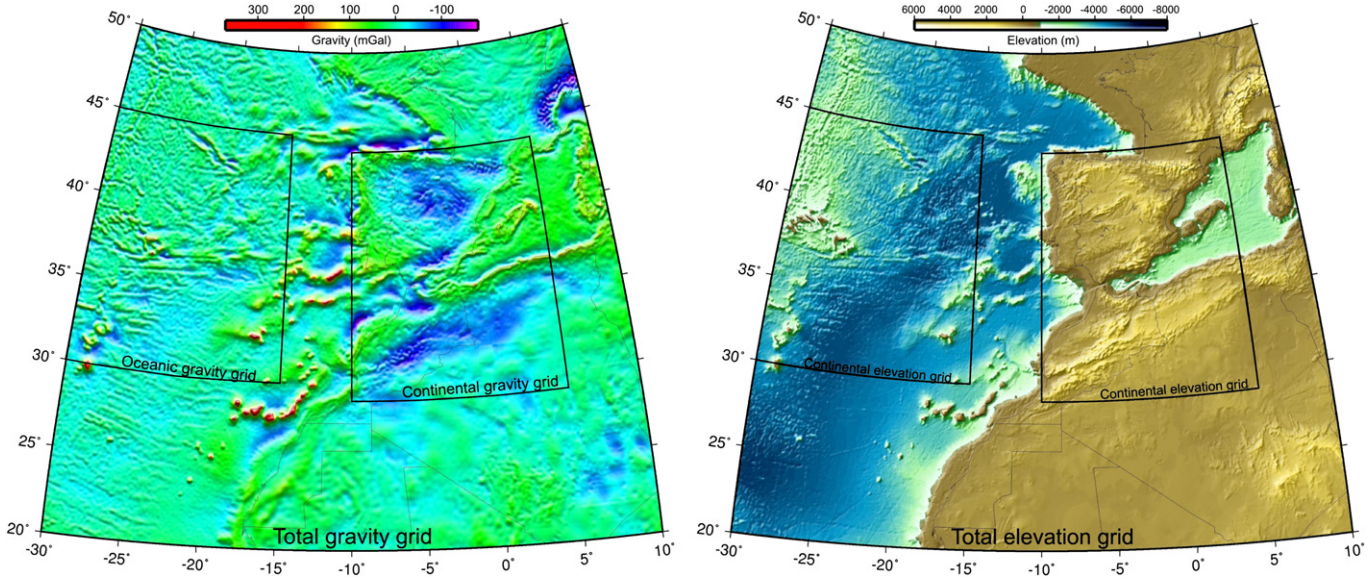

Fig. 4. Gravity anomalies and elevation maps in the study area. Black lines indicate the two zones chosen to analyze oceanic–continental lithospheric folding along the western Africa–Eurasia boundary. (For interpretation of the references to color in this figure legend, the reader is referred to the web version of this article.)

Please cite this article as: Muñoz-Martín, A., et al., Spectral analysis of the gravity and elevation along the western Africa–Eurasia plate tectonic limi..., Tectonophysics (2010), doi:10.1016/j.tecto.2010.09.036

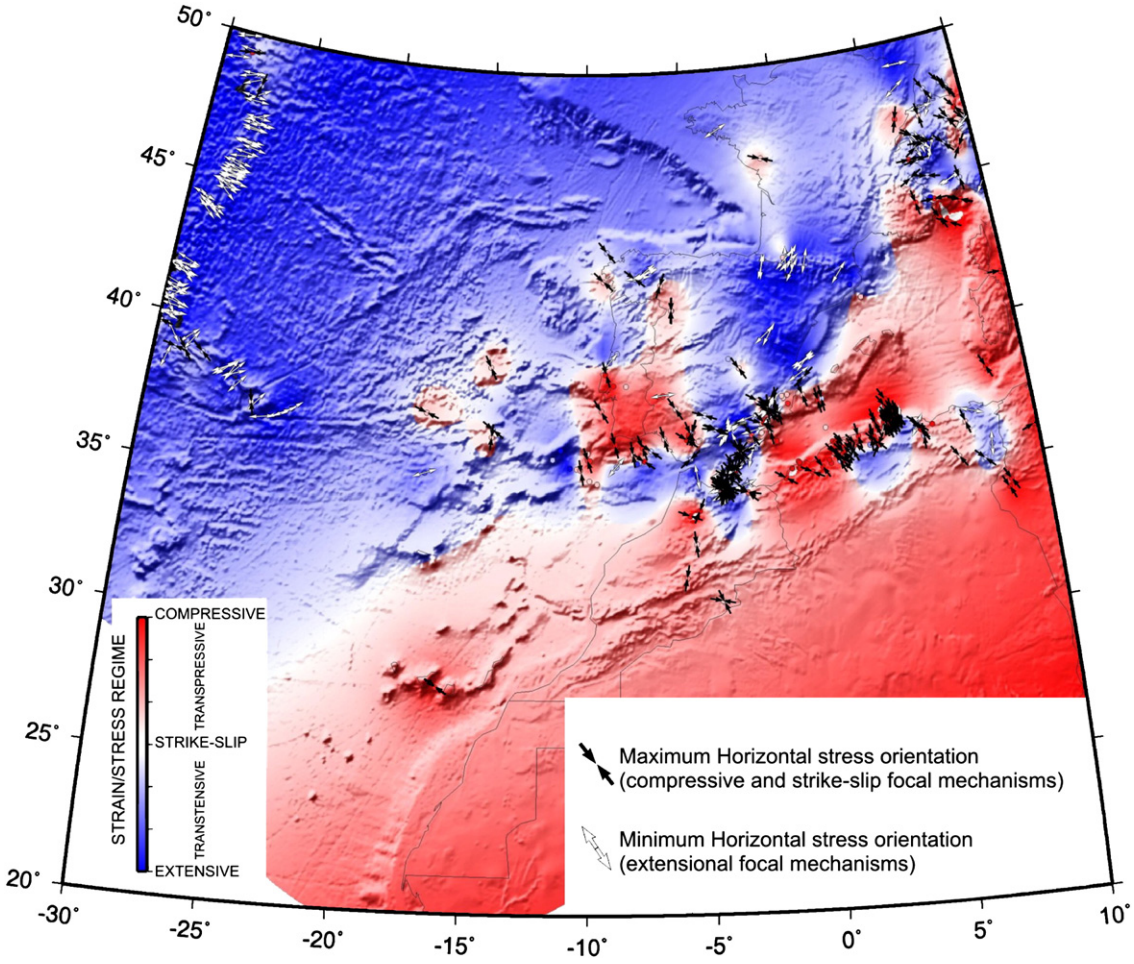

Fig. 5. Continuous strain–stress regime map for the western Africa–Eurasia plate boundary overlying topography following the methodology proposed by Olaiz et al. (2009). The individual k′ values and maximum horizontal shortening have been calculated for each focal mechanism from the "Slip Model" (Reches, 1983; De Vicente, 1988). The earthquake database is updated to December 2009 (Stich et al., 2010).

the distribution of seismic activity, there being clear concentrations of seismicity and large earthquake magnitudes where the boundary is well defined (Gorringe and N Algeria). There is also an irregular distribution of the seismicity over a wide zone (mainly at the Betics) indicating an intensely distributed deformation and probably lower earthquakes magnitudes (Figs. 1, 4, De Vicente et al., 2008; De Vicente and Vegas, 2009).

For the elevation analysis, the GEBCO (2003) data base was used for the oceanic zones and GTOPO30 for the continental zones, both re-interpolated to a 1-minute grid. The study area has two clearly defined zones which correspond to the oceanic part of both plates in the west and to the continental part in the east. In the oceanic part the topographic highs rising from the oceanic abyssal plains represent the uplifts related to the volcanic expansion axes (Canary Islands, Madeira), former expansion axes that are now inactive, banks associated with the development of the continental margin of western Iberia (Galicia Bank), as well as to compressive structures generated by a large-scale oceanic crust thrusting in the Gorringe Bank (Galindo-Zaldívar et al., 2003). What stands out in the continental part are the basement uplifts generated at the southern and northern borders of the Iberian Microplate in its collision first with Europe (Pyrenees) and later with Africa (Betics and Rif). In addition to these mountain ranges the topography shows a pattern of intraplate basement uplifts with an E–W to NE–SW orientation both in Iberia (Central System, Toledo Mountains, Sierra Morena) and in the Atlas and Anti-Atlas (Teixell et al., 2003). Another topographic feature is the basins associated with the western Mediterranean kinematics during the Neogene which caused pronounced extension in the Mediterranean margin of Iberia (Valencia Trough, Algeria–Balearic Basin).

With regard to the gravity data, the spectral analysis used data from the 1 min grav18 data base (Sandwell and Smith, 2008) in oceanic zones and gravity data from various sources (IGN, ENRESA, Bureau Gravimétrique International and Complutense University projects) in continental zones. All the data were homogenized to the same reference ellipsoid (1967), applying the free air correction to all of them and the Bouguer and topographic corrections to the continental data. Finally all data were interpolated to a gravity anomaly common grid with a resolution of 2 min.

The map of gravity anomalies obtained shows two distinct zones (Fig. 4). In the oceanic part the anomaly values are close to 0, with slightly positive and negative axes along the Atlantic Ridge, the Terceira Ridge and the ancient aborted rifts. Also noteworthy are low amplitude highs and lows associated with the oceanic crust fabric lying parallel to the transform faults. In the oceanic zone large amplitude highs are visible in the volcanic islands groups (Canary Islands and Azores), as well as in the convergent zones between oceanic lithospheres with oceanic crustal thrusting (Gorringe Bank). There are also zones of low anomaly values with large wavelengths associated with the continental margins particularly in the North of the Iberian Peninsula and in the North African–Atlantic margin. These have been interpreted as the result of the accumulation of large sedimentary sequences at the margins.

The continental zones show a distinct pattern, with a series of large gravity lows related to the main basement uplifts (Atlas, Rif, Betics

Please cite this article as: Muñoz-Martín, A., et al., Spectral analysis of the gravity and elevation along the western Africa–Eurasia plate tectonic limi..., Tectonophysics (2010), doi:10.1016/j.tecto.2010.09.036

and Pyrenees). In general these show E–W to NE–SW trends and reflect crustal thickenings caused by compressive stresses and shortening both at the boundaries and in the interior of both plates. Other minor features include the presence of low values related to the main depocenters of the major intraplate sedimentary basins (Madrid and Duero), or also to gradients associated with intracrustal lateral density contrasts (first order faults, large Variscan discontinuities etc.).

Since the results of the spectral analysis are compared in 1D and 2D in this paper, a separate analysis of the spectral signal will be undertaken, taking into account the oceanic or continental nature of the lithosphere. First of all, the study measures a series of 8 N–S profiles of which four are located in the oceanic lithosphere (Fig. 6) and four in the continental lithosphere (Fig. 7). These profiles are perpendicular to the main boundary of the plates, 2500 km in length and almost parallel to the mean shortening direction for the relative movement vectors between Africa and Eurasia during the Tertiary (Section 2, Rosenbaum et al., 2002). Four parallel E–W profiles were also obtained in order to analyze the effect of the ridge push and to compare them with the N–S profiles (Fig. 8).

Taking into account the recent change (9 My) in the Africa–Eurasia Euler vector to NW–SE (Mazzoli and Helman, 1994) and the presence of large intraplate basement uplifts with an NE–SW trend (Atlas and Spanish–Portuguese Central System), a set of 4 NW–SE profiles perpendicular to the main topographic and gravity anomalies was also measured (Fig. 10). In each case the selected profiles were of sufficient length for long wavelengths (>500 km) to be registered. These may exist in relation to large-scale lithospheric variations and so the nets are measured with a datum every 2.5 km.

For the analysis of the 2D spectral signal two zones of similar sizes ($15°\times15°$) were selected, crossed by the Africa–Eurasia plate boundary where this lies above continental and oceanic lithospheres (Fig. 4). The 2D spectral analysis in these zones included both the gravity and the elevation signals. The results from these two zones are also compared with the 2D spectrum for the whole study area ($40°\times30°$) in order to analyze the effect of the change of scale.

Finally, variograms of both gravity and elevation grids in all zones were calculated (Fig. 9) in order to determine how the anisotropy changes in relation to the tectonic characteristics (type of tectonic regime, stresses, etc.).

4. 1D spectral analysis

For all the profiles analyzed the gravity anomaly values and height are plotted against distance at the top and the normalized power spectra values (NPS) against wavelength (km) at the bottom. The spectral density values have been estimated by Welch's method of ensembling an average of multiple overlapped Windows (Welch, 1967) by means of the GMT software (Wessel and Smith, 1998). This method estimates the standard error following Bendat and Piersol (1986). The perpendicular and parallel profiles to the plate boundary are 2500 km long and have a sampling pixel of 2.5 km, with a segment size of 512.

4.1. N–S profiles across the oceanic plate boundary

Fig. 6 shows the results of the spectral analysis obtained from the 4 N–S profiles measured along the boundary between the oceanic lithospheres of Eurasia and Africa. These profiles lie completely over oceanic lithosphere from close to the Mid-Atlantic Ridge (profile A) to near the northwestern continental margin of Africa (profile D). In all of them there is a clear relationship between the gravity anomaly values and elevation. This is related with the fact that the free air anomaly used in oceanic areas is strongly dependent on bathymetry due to the high density contrast in the ocean bottom. **A** distinct change in the pattern of both profiles is visible along the plate boundary, with greater irregularity in the Eurasian oceanic lithosphere and a higher number of sea mounts and volcanic islands in the African lithosphere. The spectral analysis results show clear periodicities in all the profiles in both the gravity and elevation signals. The most frequent wavelengths are 80 ± 10 km, 150–250 km and >500 km, with these highs found in both spectrums. It is worth noting the presence of rising values of NPS in wavelengths above 1000 km in profiles A and B, which suggests the presence of longer wavelengths.

To obtain a mean value of all these 1D spectra, a stacking was carried out for the NPS values of the 4 profiles. The results show a clear correlation between the gravity and elevation data, with clear peaks in the periodicity at wavelengths of 90–100 km, 250 ± 20 km and around 650 ± 50 km. In this spectral stacking the longest periodic wavelength is best defined by the gravity data, while the shortest wavelengths are best reflected by the elevation data.

4.2. N–S profiles across the continental plate boundary

Fig. 7 shows the results for the N–S profiles perpendicular to the plate boundary calculated between both continental lithospheres, from the north of the Iberian Peninsula to the south of the Atlas Mountains in the African plate. Here, the NPS highs correspond to the gravity data with peaks in the periodicity at 90 ± 10 km, 150 km, 200–300 km and >600–700 km. In all cases the highest NPS values are found at wavelengths >300 km. Short wavelengths are best defined in the gravity spectrums, while long wavelengths are recorded in both signals. The spectrum obtained from the normalized data stacking smoothes the individual results and gives average periodic wavelengths between 80 and 90 km, 130 and 150 km and >600 km.

4.3. E–W profiles across the oceanic–continental transition

Fig. 8 shows the gravity anomaly and elevation profiles from close to the Atlantic Ridge axis to inside the Eurasia–Africa continental lithosphere. All the profiles show amplitude peaks with periodicities of 90 ± 100 km, 150–200 km and >400 km. There is a notable peak of large amplitude in profile O at the 300 km wavelength which is probably related to a series of sea mounts and volcanic islands. In all the profiles the NPS values suggest the presence of wavelengths above 1000 km that are not well defined in the spectra. In general the peak periodicities are better defined in the gravity signal, except at wavelengths over 600 km. As in the rest of the profiles analyzed, the spectrum corresponding to the stacking of these four profiles shows greater smoothing, indicating periodicities at 90–100 km, 150 km, 300 km and >600 km.

4.4. Anisotropy analysis

Given that 1D spectral analysis is sensitive to the profile orientation, an anisotropy analysis of the gravity and topographic signals was carried out for the oceanic and continental gravity and elevation grids by calculating the corresponding variograms.

The variogram is a function describing the degree of spatial dependence of a spatial random field, and allows analyzing the anisotropy of a spatial variable (Cressie, 1993). These variograms were calculated at intervals of 5° and the radial results are shown in Fig. 9 (A and C for the contact between continental lithospheres and B and D for oceanic lithospheres).

The variograms show a clear anisotropy which is more pronounced in the elevation than in the gravity owing to the potential field character of the latter, but with a strong correlation across the orientations. For the nets over the boundary between continental lithospheres, the main orientation is N65°E, and this trend remains practically the same for all wavelengths included in the grid for the gravity signal. In the case of the elevation, there is a secondary N85°E orientation for wavelengths

Please cite this article as: Muñoz-Martín, A., et al., Spectral analysis of the gravity and elevation along the western Africa–Eurasia plate tectonic limi..., Tectonophysics (2010), doi:10.1016/j.tecto.2010.09.036

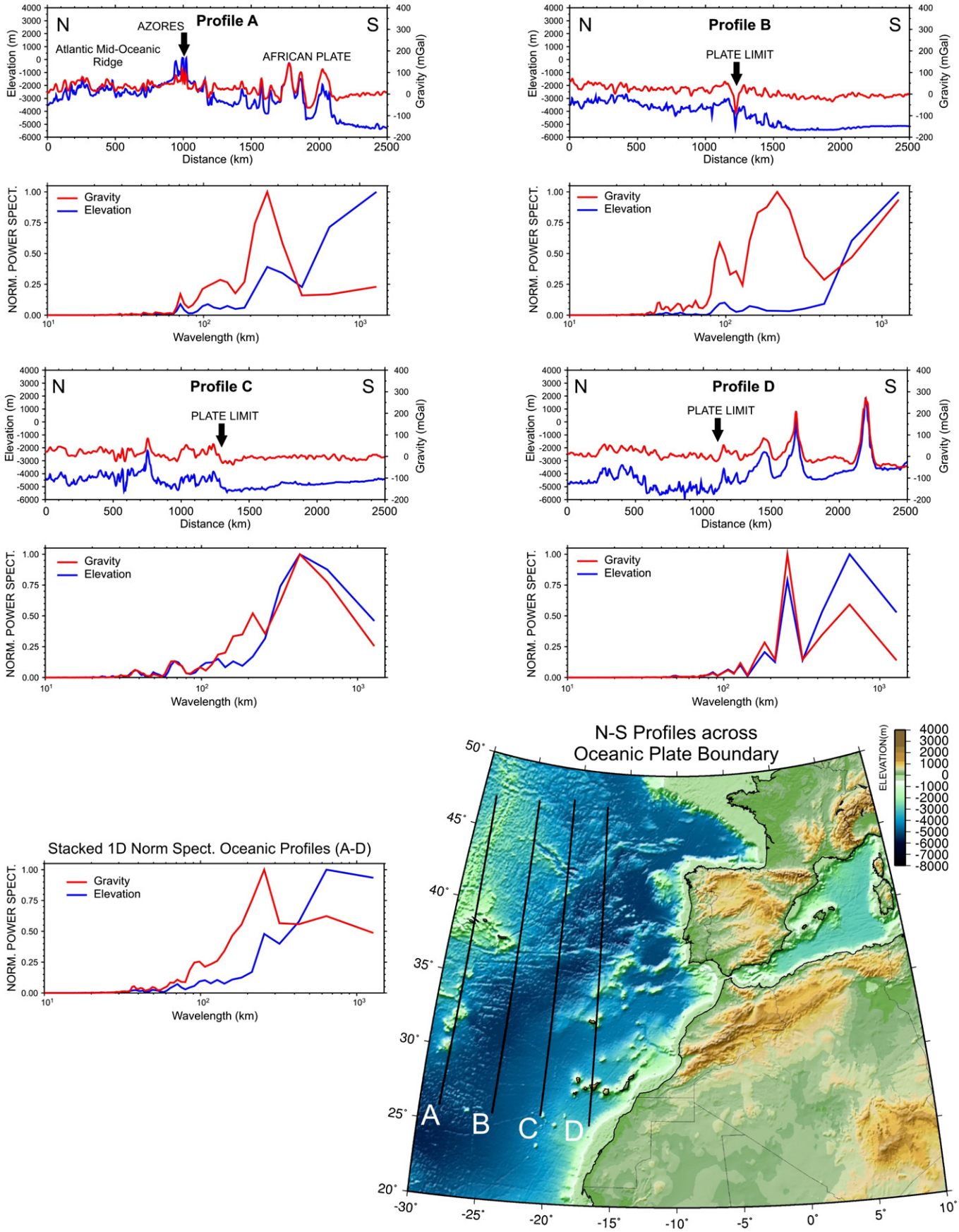

Fig. 6. Results of 1D spectral analysis of the gravity and elevation in N–S profiles perpendicular to the western Africa–Eurasia plate boundary measured between oceanic lithospheres. The elevation map shows profile location.

Please cite this article as: Muñoz-Martín, A., et al., Spectral analysis of the gravity and elevation along the western Africa–Eurasia plate tectonic limi..., Tectonophysics (2010), doi:10.1016/j.tecto.2010.09.036

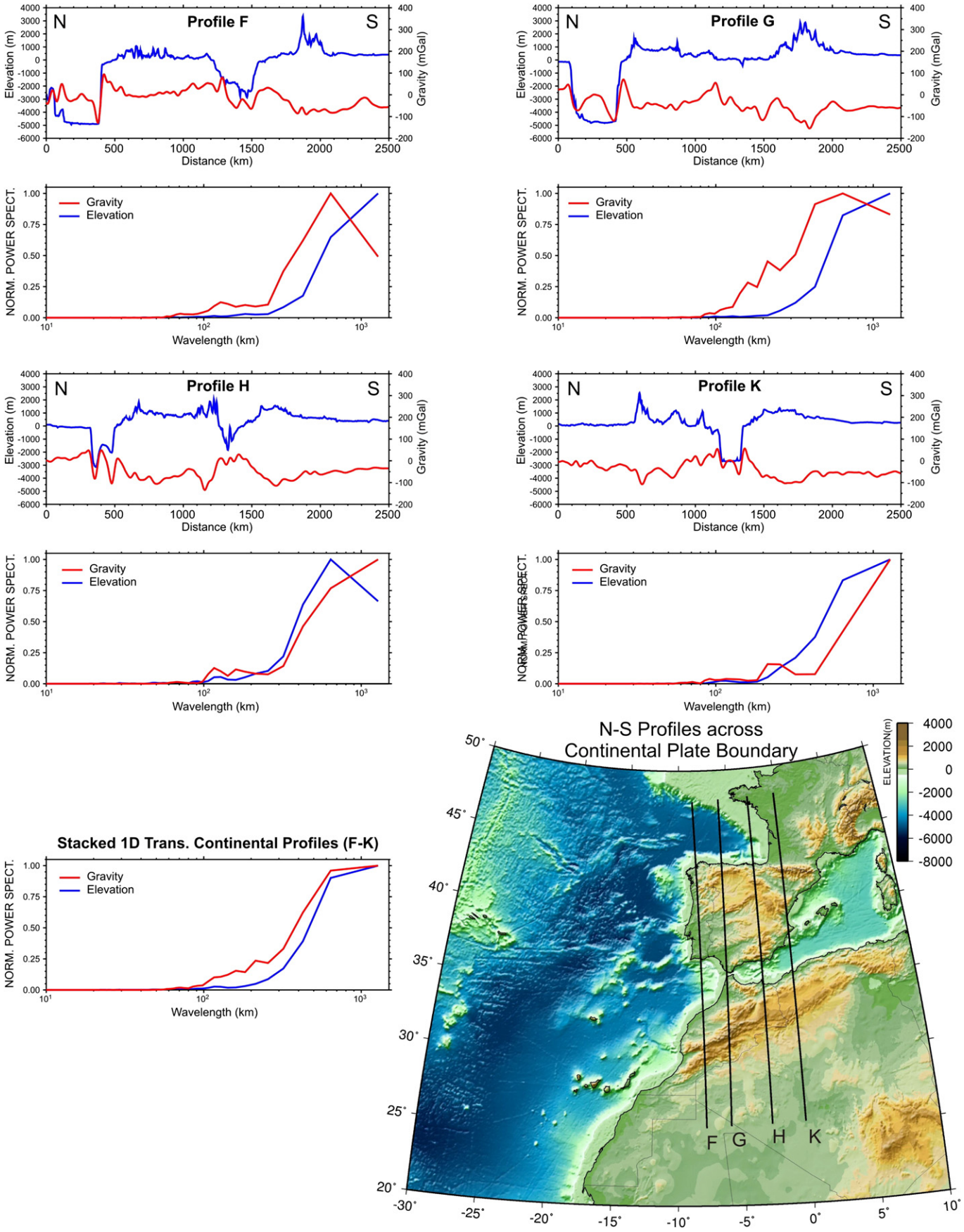

Fig. 7. Results of 1D spectral analysis of the gravity and elevation in N–S trending profiles perpendicular to the western Africa–Eurasia continental plate boundary. The elevation map shows profile location.

Please cite this article as: Muñoz-Martín, A., et al., Spectral analysis of the gravity and elevation along the western Africa–Eurasia plate tectonic limi..., Tectonophysics (2010), doi:10.1016/j.tecto.2010.09.036

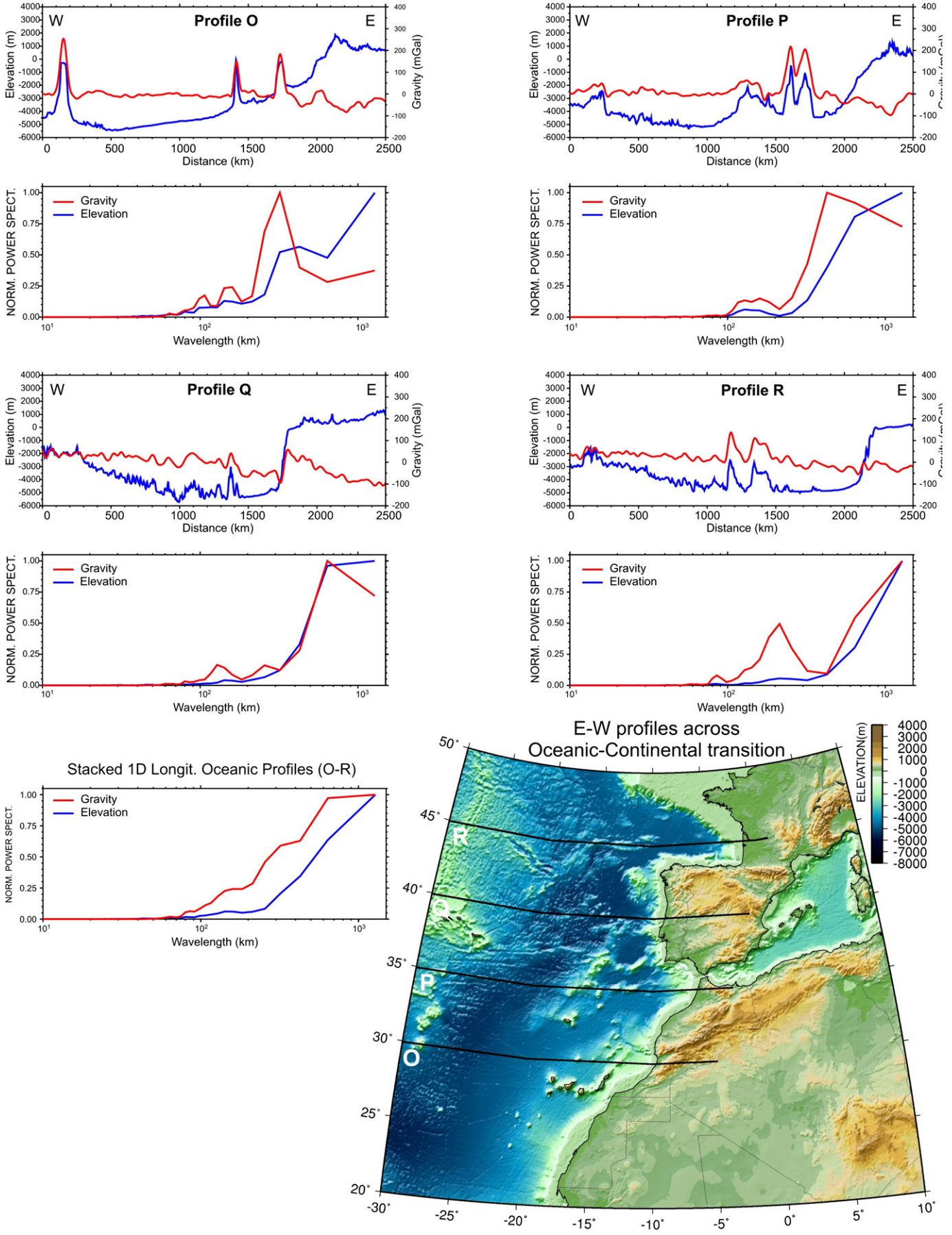

Fig. 8. Results of 1D spectral analysis of the gravity and topography in E–W trending profiles parallel to the western Africa–Eurasia plate boundary. P and Q profiles are located over the African Plate and Q and R over the Eurasian Plate. The profiles spread from close to the Atlantic Ridge to the continental margins of Africa and Europe.

Please cite this article as: Muñoz-Martín, A., et al., Spectral analysis of the gravity and elevation along the western Africa–Eurasia plate tectonic limi..., Tectonophysics (2010), doi:10.1016/j.tecto.2010.09.036

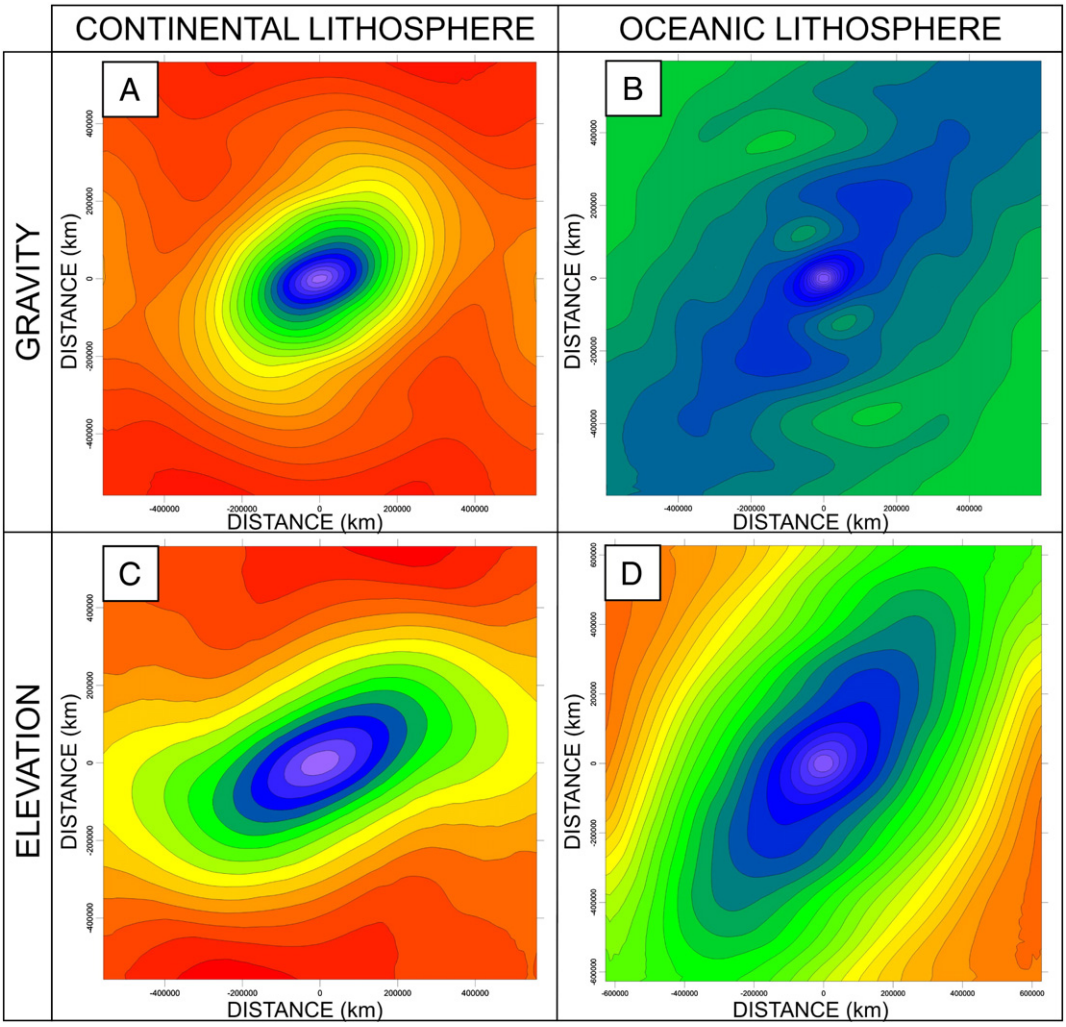

Fig. 9. Anisotropy analysis of the gravity and elevation grids by means of variograms. These variograms were calculated at intervals of 5° and the radial results are shown for the contact between continental lithospheres (A and C) and for the oceanic lithospheres (B and D). See text for further explanation.

>600 km. In contrast, for the boundary between oceanic lithospheres one can observe a main anisotropy with a direction of N37–40°E for the elevation at all wavelengths. In the case of gravity this orientation is more representative at wavelengths >300 km, whereas a N70ºE trend predominates at shorter wavelengths.

This means that the main orientations in elevation and gravity anomalies are perpendicular to the active tectonic stress trends (Müller et al., 1992; Olaiz et al., 2009; De Vicente et al., 2008), which must not have changed significantly since 9 My. These results suggest that the 1D profiles should be measured mainly in a perpendicular direction to the main anisotropy which must be obtained using a quantitative analysis.

4.5. NW–SE profiles

NW–SE profiles were also measured in order to analyze the sensitivity of the spectral analysis results to the length and orientation of the profiles, taking into account the results of the anisotropy analysis. These profiles are therefore perpendicular to the main intraplate elevation and gravity anomalies. Some were also carried out on previously published profiles (Cloetingh et al., 2002) but with improved data quality particularly for the gravity data. In addition, the length of the profiles was extended in order to analyze the effect of profile length on the spectral analysis results. The position of the profiles is perpendicular to the main tectonic structures of the zone (Gorringe Bank, Galicia Bank, Central System, and Atlas) and the results are shown in Fig. 10.

The short profiles IB1, IB2MC and IB4 (900 km long) show peaks in periodicity below 100 km, not always with a good correlation between elevation and gravity and clear spectral highs for both signals at wavelengths of 150–200 km. The IB1 and IB2MC profiles also suggest wavelengths in excess of 600 km.

The two longest profiles (IB3 and IB2L of 2500 km in length) show periodicities below 100 km in the IB3, and in both cases signal peaks between 150 and 200 km. There are maximum NPS values for wavelengths longer than 600 km. In the IB2L profile, however, the gravity points to an even longer wavelength.

As for the change in periodicities in relation to the profile length, profile IB2MC (900 km) was extended in two different profiles (IB2L and IB2ML of 1500 and 2500 km respectively) with the same starting point and orientation. The results show that with a longer profile, wavelengths below 100 km disappear in the gravity and elevation NPS, while wavelengths of 200 ± 50 km become more stable in line with the previous results (Cloetingh et al., 2002). There is also a peak of more than 500 km of wavelength in the three profiles.

5. 2D spectral analysis

The NPS calculation in 2D was applied to both zones crossed by the plate boundary between Eurasia and Africa, where this is developed over oceanic and continental lithosphere (Fig. 3), as well as to the

Please cite this article as: Muñoz-Martín, A., et al., Spectral analysis of the gravity and elevation along the western Africa–Eurasia plate tectonic limi..., Tectonophysics (2010), doi:10.1016/j.tecto.2010.09.036

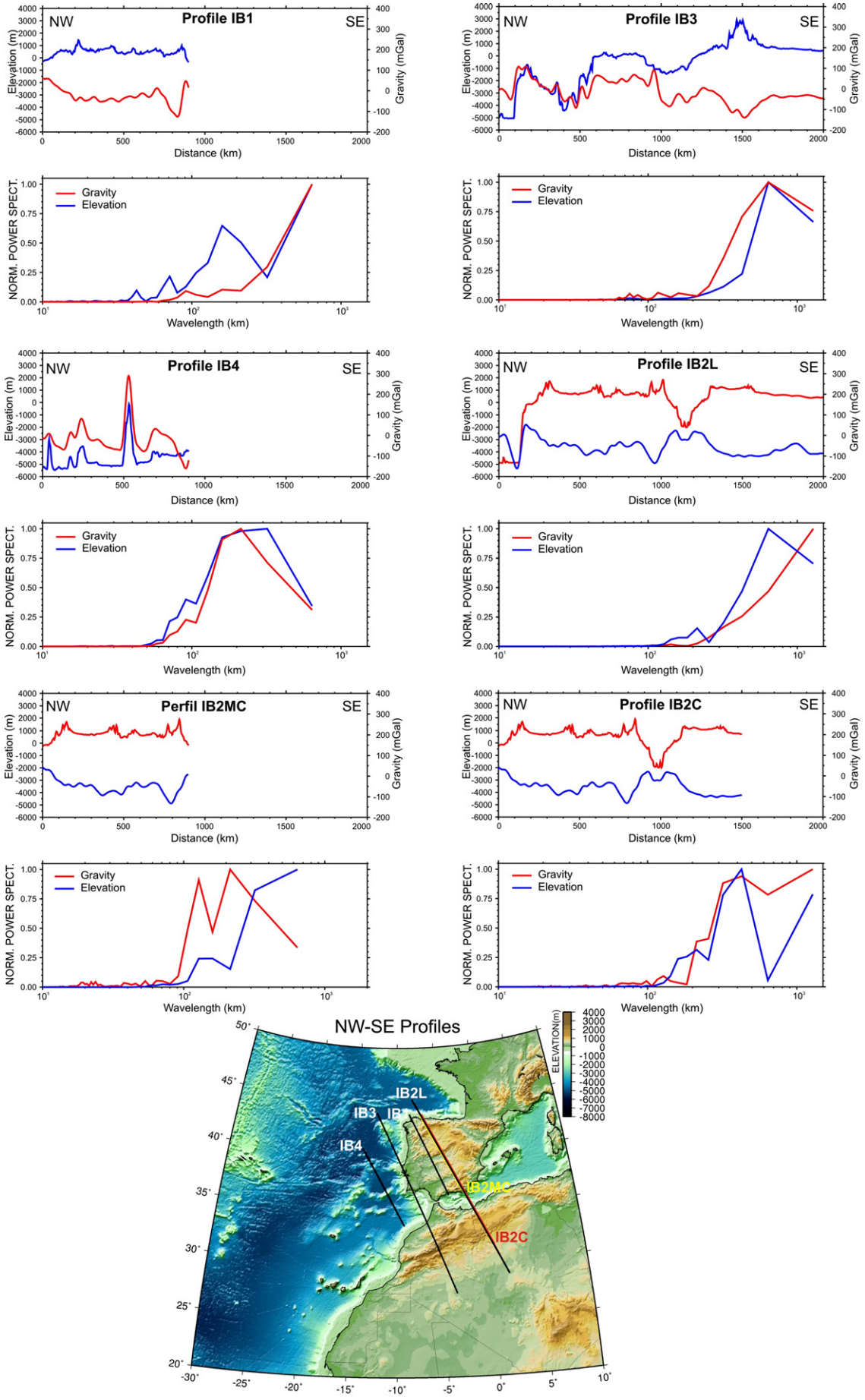

Please cite this article as: Muñoz-Martín, A., et al., Spectral analysis of the gravity and elevation along the western Africa–Eurasia plate tectonic limi..., Tectonophysics (2010), doi:10.1016/j.tecto.2010.09.036

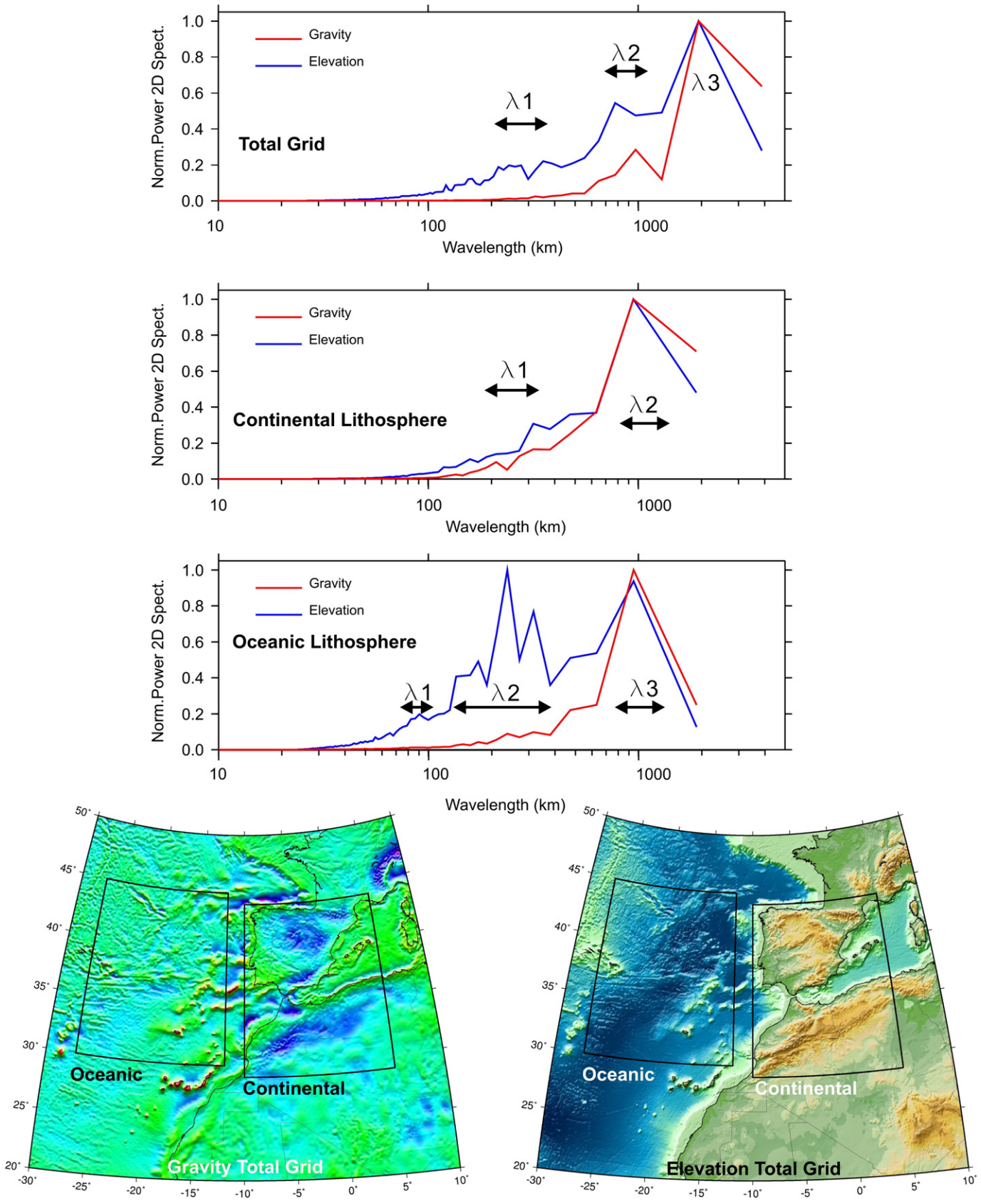

Fig. 11. 2D spectral analysis results calculated from gravity and elevation total grids, as well as from the areas located over the limit between oceanic and continental lithospheres. Main periodic wavelengths are marked. See text for discussion.

Fig. 10. Results of 1D spectral analysis of the gravity and elevation in NW–SE trending profiles perpendicular to the main gravity and elevation anisotropy and parallel to the active SHMAX orientations (De Vicente et al., 2008). See text for further explanation.

Please cite this article as: Muñoz-Martín, A., et al., Spectral analysis of the gravity and elevation along the western Africa–Eurasia plate tectonic limi..., Tectonophysics (2010), doi:10.1016/j.tecto.2010.09.036

complete gravity and elevation grids (40°×30°). The results are shown in Fig. 11. In the case of the boundary between continental lithospheres the spectral analysis shows peaks at 150–200 km, one at 300 km and a maximum wavelength of 900±50 km. In this case the gravity signal has NPS values that are more similar to those of the elevation signal. The results for the boundary between oceanic lithospheres show a more complex spectrum, there being clear signal highs at 90±10 km and 150–300 km, and another peak at 900± 50 km. All these periodicities are also visible, though less clearly, in the gravity signal.

For the whole surface area analyzed, the elevation spectrum shows clear signal highs at 200–350 km, 900±100 km and an absolute maximum peak at 2000 km. There are also other shorter-wavelength periodicities, though these have low NPS values and are more clearly defined for elevation than for gravity. There is only a clear correlation between both signals at wavelengths over 200 km.

5.1. Analysis of the 2D spectral analysis results

Wavelengths longer than 600 km are excluded from the theoretical models that relate lithospheric folding with thermo-tectonic age of the lithosphere (Cloetingh et al., 1999), leaving their meaning enigmatic. In order to understand these signals better, the grids corresponding to elevation and gravity have been filtered, thereby mapping these variations (Fig. 12). To do so, the anomalies that may be associated with lithospheric folding (wavelengths from 100 to 600 km) and those with wavelengths over 700 km have been filtered out. Fig. 11 shows the maps of anomalies for wavelengths between 100 and 600 km at the boundary between oceanic and continental lithospheres, as well as the gravity and elevation signals with wavelengths of 700 to 1200 km. In the first case the variations are related to lithosphere-scale structures and to changes in crustal thickness associated with the development of mountain chains (in the case of the continental lithosphere). The pattern in the oceanic lithosphere is less clear and shows an NNE–SSW trend probably associated with variations in the lithosphere structure linked to the Mid-Atlantic Ridge (Müller et al., 2008). This fact is clearer near the ridge, and it could be related with a decreasing in the elastic thickness near the ridge due to a higher geothermal gradient.

The variations in the elevation anomalies with wavelengths over 700 km coincide with the transition from oceanic to continental crust, as well as with the development of the Mid-Atlantic Ridge. The gravity pattern is less clear, but the gravity signal at wavelengths between 700 and 1200 km seems to be connected with the regional component (<2000 km) of the residual mantle anomalies of the gravity field obtained after removal of the crustal effect from the observed field (Tesauro et al., 2007).

One unexpected aspect is the presence of 2000 km wavelengths in both signals when the whole grid is analyzed in 2D. The projection of these filtered anomalies shows a similar association with the main boundary macrostructures as the 700 to 1200 km wavelengths, and probably are the result of the net size itself chosen for the analysis (aliasing effect).

6. Discussion and conclusions

The spectral analysis of 1D topographic and gravity profiles is a useful tool to quantify periodic signals, but the results are highly dependent on the profile location, orientation and length, and also to a lesser extent on the sampling interval. For detecting elevation and/or gravity periodic signals from profiles, it is then necessary: A) to draw variograms from 2D data to determine the main anisotropies and measure the profiles perpendicularly; B) to check that the length of the measuring profile is double that of the analyzed periodic signal; and C) to make sure that different sampling intervals do not excessively distort the spectral results.

The 2D spectral analysis avoids the problems found in relation to the particular location of the profile but the resulting wavelengths are slightly higher than those obtained from the 1D spectral analysis (Fig. 13). This occurs because radial calculation averages the real anisotropy values present in the signal. However, 2D spectral analysis allows the filtering of the different signals in order to map out the periodicities and undertake a precise spatial interpretation, not only a qualitative one. Our analysis confirms that the results of spectral analysis generally produce a periodic signal that depends on the size of the profile or selected net. It is then essential to check that the periodic signals detected remain when the length of the profile or the net size is increased or whether the position of the profile changes.

Our results indicate that the greater the profile length, the longer the wavelength peaks that are found. Nevertheless, there are some periodic signals that appear in almost all the analyzed profiles. The most frequent are signals with wavelengths of 100 and 250 km for the profiles perpendicular to the plate boundary between oceanic lithospheres. Where the plate boundary is developed over continental lithospheres the most frequent wavelengths are between 150 and 250 km. This fact implies the presence of lithospheric folds in both the oceanic and continental crusts all along the boundary between the Eurasian and African plates from Iberia to the Azores triple junction. The development of lithospheric folding results in the coupling of both lithospheres, as had already been put forward for Iberia (Cloetingh et al., 2002), but not for the boundary between S Iberia and the Azores triple junction. It is worth noting that the orientation of these folds changes from NE–SW at the Iberia–Africa contact to NNE–SSW at the contact of the continental lithospheres (Figs. 9, 12). These orientations are compatible with and perpendicular to the S_{HMAX} trend of the zone, which is also found to rotate in an anticlockwise direction (De Vicente et al., 2008).

In the case of the N–S profiles along the boundary between oceanic lithospheres, wavelengths are found to lengthen from west to east. This trend reflects the increase in the age of the oceanic lithospheres in the same direction (McAdoo and Sandwell, 1985; Müller et al., 2008). The degree of dispersion observed in the determination of the oceanic lithosphere age is due to the fact that the profiles are oblique to the isochrones of the oceanic floor and cross the boundary between the two plates. In addition, the wavelengths calculated with the 1D profiles are slightly lower than those obtained using 2D, which give an average between 150 and 300 km. These values correspond to an elasto-plastic oceanic lithosphere with sediment loading >50 My (McAdoo and Sandwell, 1985).

Previous studies show duplicity in the periodic signals of those cases of continental deformation when there is a decoupling between the upper crust and the lithosphere mantle, with wavelengths for the upper structural level <100 km. The profiles analyzed show periodicities of wavelengths within this range in both types of lithospheres but with a high dispersion in the NPS values. The highest NPS values are observed in the oceanic lithosphere and/or when the continental lithosphere profiles are shorter and perpendicular to the anomaly. It is also noteworthy that the signal peaks disappear in the 2D spectra at wavelengths below 100 km. This relatively low amplitude in the continental lithosphere has been interpreted in the case of Iberia as the result of erosion processes (Cloetingh et al., 2002), which explains the larger amplitudes detected in oceanic profiles. Moreover, the variation in the relative amplitude of the short wavelengths must be controlled by the structure and proprieties of the upper crust in each case.

Fig. 12. Filtered maps of elevation and gravity anomalies for wavelengths between 100 and 600 km at the limit between oceanic and continental lithospheres. The bottom maps show main gravity anomaly and elevation signals with wavelengths >700 km for the whole study zone. See text for discussion.

Please cite this article as: Muñoz-Martín, A., et al., Spectral analysis of the gravity and elevation along the western Africa–Eurasia plate tectonic limi..., Tectonophysics (2010), doi:10.1016/j.tecto.2010.09.036

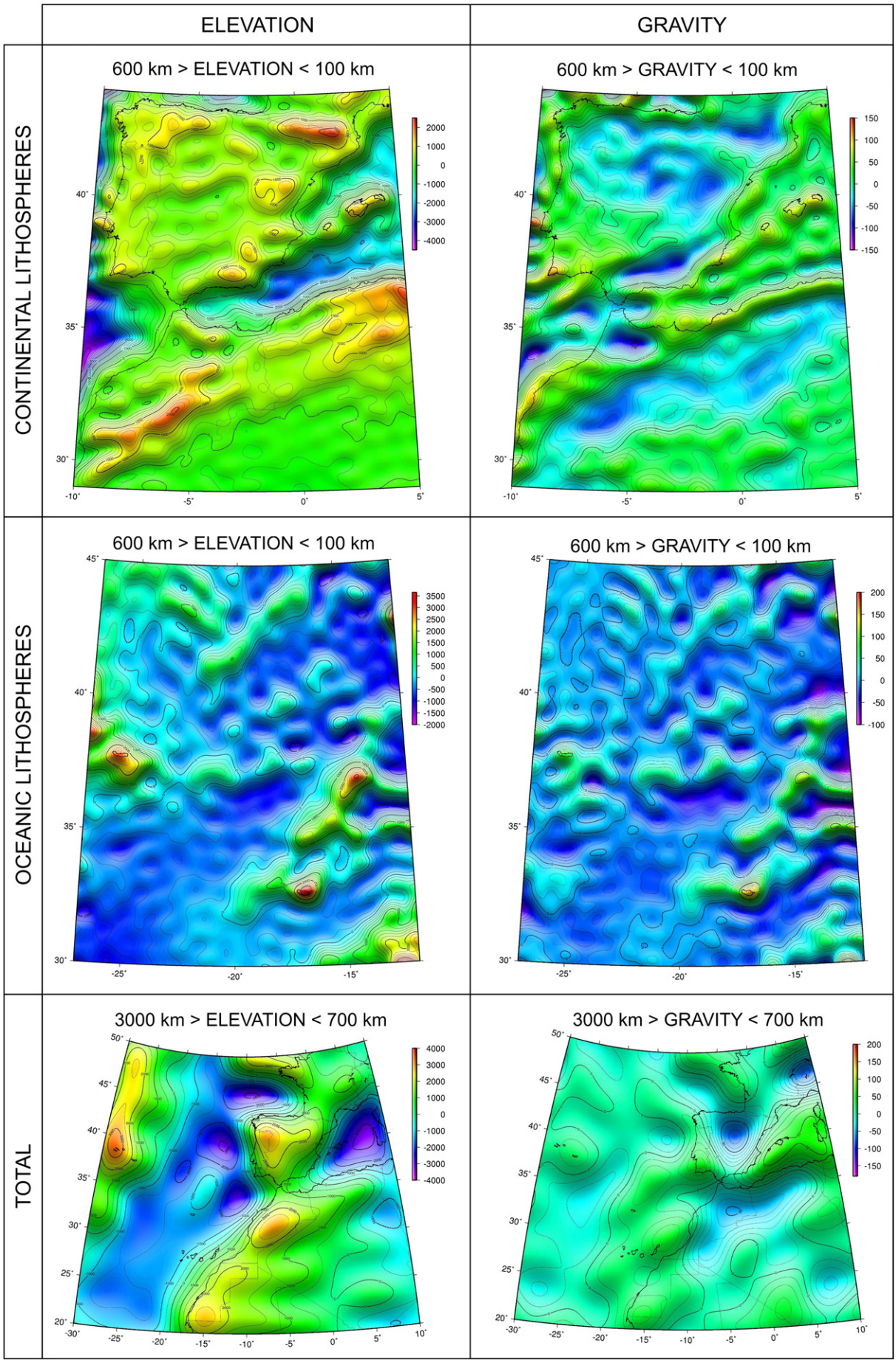

Please cite this article as: Muñoz-Martín, A., et al., Spectral analysis of the gravity and elevation along the western Africa–Eurasia plate tectonic limi..., Tectonophysics (2010), doi:10.1016/j.tecto.2010.09.036

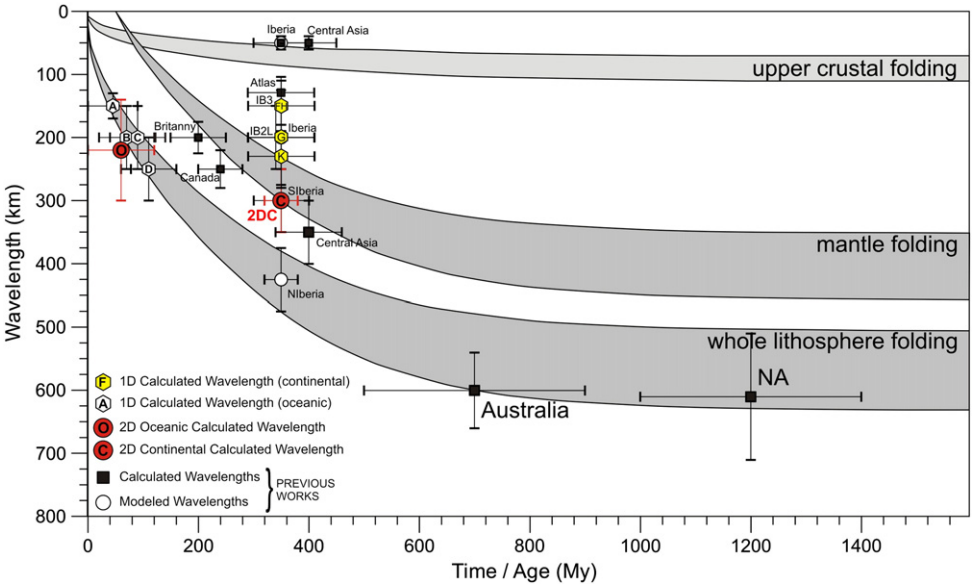

Fig. 13. Comparison of previously observed (solid squares) and modeled (open circles) wavelengths with 1D and 2D wavelengths calculated in this work. Previous studies include models and theoretical predictions (open circles, Cloetingh et al., 1999, 2002) and other estimates (black squares) for wavelengths documented from geological and geophysical studies (Stephenson and Cloetingh, 1991; Lambeck, 1983; Ziegler et al., 1995; Nikishin et al., 1993; Bonnet et al., 2000; Teixell et al., 2003). There is a clear relationship between lithospheric wavelength and age for 1D oceanic profiles (A–D). Wavelengths calculated in 2D are slightly longer than those calculated in 1D (see text for discussion). (For interpretation of the references to color in this figure legend, the reader is referred to the web version of this article.)

The dominant wavelengths in the lithospheric folding depend on the mantle strength (Sokoutis et al., 2005; Schmalholz et al., 2009), the thermo-tectonic age of the lithosphere (McAdoo and Sandwell, 1985; Cloetingh and Burov, 1996), the intensity of the deformation and the coupling/decoupling between the upper crust and the mantle in the case of the continental lithosphere (Cloetingh et al., 1999) or between different lithospheres (Willingshofer and Sokoutis, 2009). In our case, the wavelengths calculated for the boundary between continental lithospheres (<250 km) suggest low mean mantle strength values ($<10^{13}$ Pa m, Sokoutis et al., 2005). These values coincide with the mean integrated strength values estimated under conditions of compression as calculated by Tesauro et al. (2009) for the continental lithosphere in Iberia.

Finally, a large periodic signal (wavelength >600 km) was also detected. After drawing the filtered values (Fig. 12), the resulting maps indicate that this signal is related to the transition between continental and oceanic lithospheres and to the significant changes in crustal and/or lithospheric thickness from the Mid-Atlantic Ridge to the continental margins of western Eurasia (Tesauro et al., 2009). The gravity signal at wavelengths between 700 and 1200 km has no direct relationship with the lithospheric structure, but seems to be connected with the regional component (<2000 km) of the residual mantle anomalies of the gravity field obtained after the removal of the crustal effect from the observed field (Tesauro et al., 2007).

Acknowledgements

This study was supported by Consolider Ingenio 2006 "Topo Iberia" CSD2006-00041 and the Spanish National Research Program CGL2006-13926-C02-01-02 "Topo Iberia Foreland". The GMT software system from Wessel and Smith (1998) was invaluable for drawing the figures and to calculate 1D and 2D NPS. We appreciate the comments of the anonymous reviewers and the editor, which help to focus and to improve the manuscript.

References

Andeweg, B., De Vicente, G., Cloetingh, S., Giner, J., Muñoz Martin, A., 1999. Local stress fields and intraplate deformation of Iberia: variations in spatial and temporal interplay of regional stress sources. Tectonophysics 305 (1–3), 153–164.

Beekman, F., Bull, J.M., Cloetingh, S., Scrutton, R.A., 1996. Crustal fault reactivation facilitating lithospheric folding/buckling in the central Indian Ocean. Geol. Soc. Spec. Publ. 99, 251–263.

Bendat, J.S., Piersol, A.G., 1986. Random Data: Analysis and Measurement Procedures, second ed. John Wiley & Sons Inc.

Bonnet, S.F., Guillocheau, F., Brun, J.P., Van den Driessche, J., 2000. Large-scale relief development related to Quaternary tectonic uplift of a Proterozoic–Paleozoic basement: the Armorican Massif, NW France. J. Geophys. Res. 105, 19273–19288.

Braunmiller, J., Kradolfer, U., Baer, M., Giardini, D., 2002. Regional moment-tensor inversion in the European–Mediterranean area—initial results. Tectonophysics 356, 5–22.

Burov, E.B., Cloetingh, S., 1997. Erosion and rift dynamics: new thermo-mechanical aspects of post-rift evolution of extensional basins. Earth Planet. Sci. Lett. 150, 7–26.

Burov, E.B., Poliakov, A.N.B., 2001. Erosion and rheology controls on synrift and postrift evolution: verifying old and new ideas using a fully coupled numerical model. J. Geophys. Res. 106, 16461–16481.

Cloetingh, S., Burov, E.B., 1996. Thermomechanical structure of European continental lithosphere: constraints from rheological profiles and EET estimates. Geophys. J. Int. 124, 695–723.

Cloetingh, S., Burov, E.B., Poliakov, A., 1999. Lithosphere folding: primary response to compression? (from central Asia to Paris basin). Tectonics 18 (6), 1064–1083.

Cloetingh, S., Burov, E., Beekman, F., Andeweg, B., Andriessen, P., García-Castellanos, D., De Vicente, G., Vegas, R., 2002. Lithospheric folding in Iberia. Tectonics 21 (5), 1041–1067.

Cressie, N., 1993. Statistics for Spatial Data. Wiley, NY. 900 pp.

de Lamotte, D., et al., 2009. Mesozoic and Cenozoic vertical movements in the Atlas system (Algeria, Morocco, Tunisia): an overview. Tectonophysics 475 (1), 9–28.

De Vicente, G., 1988. Análisis poblacional de fallas. El sector de enlace Sistema Central-Cordillera Ibérica. PhD Thesis. Univ. Complutense de Madrid. 317 p.

De Vicente, G., Vegas, R., 2009. Large-scale distributed deformation controlled topography along the western Africa–Eurasia limit: tectonic constraints. Tectonophysics 474, 124–143.

De Vicente, G., Cloetingh, S., Muñoz-Martín, A., Olaiz, A., Stich, D., Vegas, R., Galindo-Zaldivar, J., Fernández-Lozano, J., 2008. Inversion of moment tensor focal mechanisms for active stresses around Microcontinent Iberia: tectonic implications. Tectonics 27, 1–22.

Dziewonski, A.M., Woodhouse, J.H., 1983. An experiment in the systematic study of global seismicity: centroid moment-tensor solutions for 201 moderate and large earthquakes of 1981. J. Geophys. Res. 88, 3247–3271.

Dziewonski, A.M., Chou, T.A., Woodhouse, J.H., 1982. Determination of earthquake source parameters from waveform data for studies of global and regional seismicity. J. Geophys. Res. 86, 2825–2852.

Fernández-Lozano, J. Sokoutis, D., Willingshofer, E. De Vicente, G., Cloetingh, S., in press. Analogue modelling: insights on lithospheric processes in Iberia. doi:10.1029/2010TC002719.

Fullea, J., Fernàndez, M., Afonso, J.C., Vergés, J., Zeyen, H., in press. The structure and evolution of the lithosphere–asthenosphere boundary beneath the Atlantic–Mediterranean Transition Region. Lithos doi:10.1016/j.lithos.2010.03.003.

Galindo-Zaldívar, J., Maldonado, A., Schreider, A.A., 2003. Gorringe Ridge gravity and magnetic anomalies are compatible with thrusting at a crustal scale. Geophys. J. Int. 153, 586–594.

García-Castellanos, D., 2002. Interplay between lithospheric flexure and river transport in foreland basins. Basin Res. 14, 89–104.

GEBCO, 2003. IHO-UNESCO, General bathymetric chart of the oceans, digital edition, http://www.ngdc.noaa.gov/mgg/gebco.
Gerbault, M., 1999. At what stress level is the central Indian Ocean buckling? Earth and Planetary Science Letters 178, p. 165–181.
Ghorbal, B., Bertotti, G., Foeken, J., Andriessen, P., 2008. Unexpected Jurassic to Neogene vertical movements in 'stable' parts of NW Africa revealed by low temperature geochronology. Terra Nova 00, 1–9 doi:10.1111/j.1365-3121.2008.00828.x.
International Seismological Centre, 2009, EHB Bulletin, http://www.isc.ac.uk, Internatl. Seis. Cent., Thatcham, United Kingdom.
Krishna, K.S., Bull, J.M., Scrutton, R.A., 2001. Evidence for multiphase folding of the central Indian Ocean lithosphere. Geology 29 (8), 715–718.
Lambeck, K., 1983. The role of compressive forces in intracratonic basin formation and mid-plate orogenies. Geophys. Res. Lett. 10, 845–848.
Luth, S., Willingshofer, E., Sokoutis, D., Cloetingh, D., 2010. Analogue modelling of continental collision: influence of plate coupling on mantle lithosphere subduction, crustal deformation and surface topography. Tectonophysics 484, 87–102 doi:10.1016/j.tecto.2009.08.043.
Martinod, J., Davy, P., 1994. Periodic instabilities during compression of the lithosphere, 2, Analogue experiments. J. Geophys. Res. 99, 57–69.
Mazzoli, S., Helman, M., 1994. Neogene patterns of relative plate motions for Africa–Europe: some implications for recent central Mediterranean tectonics. Geol. Rundsch. 83, 464–468.
McAdoo, D.C., Sandwell, D.T., 1985. Folding of oceanic lithosphere. J. Geophys. Res. 90 (B10), 8563–8569.
Müller, B., Zoback, M.L., Fuchs, K., Mastin, L.G., Gregersen, S., Pavoni, N., Stephansson, O., Ljunggren, L., 1992. Regional patterns of tectonic stress in Europe. J. Geophys. Res. 97, 11783–11803.
Müller, R.D., Sdrolias, M., Gaina, C., Roest, W.R., 2008. Age, spreading rates, and spreading asymmetry of the world's ocean crust. Geochem. Geophys. Geosyst. 9, Q04006.
Nikishin, A.M., Cloetingh, S., Lobkovsky, L., Burov, E.B., 1993. Continental lithosphere folding in central Asia, part I, constraints from geological observations. Tectonophysics 226, 59–72.
Olaiz, A.J., Muñoz-Martín, A., De Vicente, G., Vegas, R., Cloetingh, S., 2009. European continuous active tectonic strain–stress map. Tectonophysics 474, 33–40.
Palencia, A., (2004) Estudio paleomagnético de rocas de edad jurásica en la Península Ibérica y en el sur de Marruecos. Ph.D.Thesis. Universidad Complutense de Madrid 275 pp.
Pondrelli, S., Morelli, A., Ekström, G., Mazza, S., Boschi, E., Dziewonski, M., 2002. European–Mediterranean regional centroid-moment tensors: 1997–2000. Phys. Earth Planet. Inter. 130, 71–101.
Pondrelli, S., Morelli, A., Ekström, G., 2004. European–Mediterranean regional centroide moment tensor catalog: solutions for years 2001 and 2002. Phys. Earth Planet. Inter. 145, 127–147.
Ranalli, G., 1995. Rheology of the Earth. Kluwer Academic Publishers.
Reches, Z., 1983. Faulting of rocks in three-dimensional strain fields. II Theoretical analysis. Tectonophysics 47, 109–129.
Rosenbaum, R., Lister, G.S., Duboz, C., 2002. Relative motions of Africa, Iberia and Europe during Alpine orogeny. Tectonophysics 359, 117–129.
Rueda, J., Mezcua, J., 2005. Near-real-time seismic moment-tensor determination in Spain. Seismol. Res. Lett. 76 (4), 455–465.
Sandwell, D.T., Smith, W.H.F., 2008. Global marine gravity from retracked Geosat and ERS-1 altimetry: ridge Segmentation versus spreading rate. J. Geophys. Res. 114, B01411.
Schmalholz, S., Podladchikov, Y., Burg, J., 2002. Control of folding by gravity and matrix thickness: implications for large-scale folding. J. Geophys. Res. Solid Earth 107 (B1) doi:10.1029/2001JB000355.
Schmalholz, S.M., Kaus, B.J.P., Burg, J.P., 2009. Stress–strength relationship in the lithosphere during continental collision. Geology 37 (9), 775–778.
Serpelloni, E., Vannucci, G., Pondrelli, S., Argnani, A., Casula, G., Anzidei, M., Baldi, P., Gasperini, P., 2007. Kinematics of theWestern Africa–Eurasia plate boundary from focal mechanisms and GPS data. Geophys. J. Int. 169, 1180–1200.
Sokoutis, D., Burg, J.P., Bonini, M., Corti, G., Cloetingh, S., 2005. Lithospheric-scale structures from the perspective of analogue continental collision. Tectonophysics 406, 1–15.
Sonder, L., England, P., 1986. Vertical averages of rheology of the continental lithosphere: relation to thin sheet parameters. Earth Planet. Sci. Lett. 77 (1), 81–90.
Stapel, G., 1999. The nature of isostasy in West Iberia and its bearing on Mesozoic and Cenozoic regional tectonics. Published PhD thesis, Vrije Universiteit Amsterdam, the Netherlands.
Stephenson, R.A., Cloetingh, S., 1991. Some examples and mechanical aspects of continental lithospheric folding. Tectonophysics 188, 27–37.
Stich, D., Ammon, C.J., Morales, J., 2003. Moment tensor solutions for small and moderate earthquakes in the Ibero–Maghreb region. J. Geophys. Res. 108, 02JB002057.
Stich, D., Martín, R., Morales, J., 2010. Moment tensor inversion for Iberia–Maghreb earthquakes 2005–2008. Tectonophysics 390–398.
Stuwe, K., 2007. Geodynamics of the Lithosphere, 2nd ed. Springer-Verlag, Berlin, Heidelberg, Dordrecht. 493 pp.
Teixell, A., Arboleya, M.L., Julivert, M., Charroud, M., 2003. Tectonic shortening and topography in the central High Atlas (Morocco). Tectonics 22 (5), 1051.
Tejero, R., Ruiz, J., 2002. Thermal and mechanical structure of the central Iberian Peninsula lithosphere. Tectonophysics 350 (1), 49–62.
Tesauro, M., Kaban, M.K., Cloetingh, S., Hardebol, N.J., Beekman, F., 2007. 3D strength and gravity anomalies of the European lithosphere. Earth Planet. Sci. Lett. 263, 56–73.
Tesauro, M., Kaban, M.K., Cloetingh, S., 2008. EuCRUST-07: a new reference model for the European crust. Geophys. Res. Lett. 35 (L05313), 5 pp. doi:10.1029/2007GL032244.
Tesauro, M., Kaban, M.K., Cloetingh, S., 2009. A new thermal and rheological model of the European lithosphere. Tectonophysics 476, 478–495.
Vázquez, J.T., Vegas, R., 2000. Acomodación de la convergencia entre África y la Península Ibérica, Golfo de Cádiz y Mar de Alborán, a partir de del análisis de terremotos. Geogaceta 27, 171–174.
Verges, J., Fernandez, M., 2006. Ranges and basins in the Iberian Peninsula: their contribution to the present topography. Mem. Geol. Soc. Lond. 32, 223–234.
Welch, P.D., 1967. The use of fast fourier transform for the estimation of power spectra: a method based on time averaging over short, modified periodograms. IEEE Trans. Audio Electroacoust. AU-15, 70–73.
Wessel, P., Smith, W.H.F., 1998. New, improved version of Generic Mapping Tools released. Eos Trans. AGU 79, 579.
Willingshofer, E., Sokoutis, D., 2009. Decoupling along plate boundaries: key variable controlling the mode of deformation and the geometry of collisional mountain belts. Geology 37, 39–42.
Ziegler, P.A., Cloetingh, S., Van Wees, J.D., 1995. Geodynamics of intraplate compressional basin deformation: the Alpine foreland and other examples. Tectonophysics 252, 7–59.

Please cite this article as: Muñoz-Martín, A., et al., Spectral analysis of the gravity and elevation along the western Africa–Eurasia plate tectonic limi..., Tectonophysics (2010), doi:10.1016/j.tecto.2010.09.036